Concanamycin and Indolyl Pentadieneamide Inhibitors of the Vacuolar H^+-ATPase Bind with High Affinity to the Purified Proteolipid Subunit of the Membrane Domain†

Graham Whyteside,‡ Peter J. Meek,‡ Stephen K. Ball,‡ Neil Dixon,§ Malcolm E. Finbow,|| Terence P. Kee,§ John B. C. Findlay,‡ and Michael A. Harrison*,‡

School of Biochemistry and Microbiology and School of Chemistry, University of Leeds, Woodhouse Lane, Leeds LS2 9JT, U.K., and School of Biomedical Sciences, Glasgow Caledonian University, Glasgow G4 0BA, U.K.

Received August 1, 2005; Revised Manuscript Received September 19, 2005

ABSTRACT: The macrolide antibiotic concanamycin is a potent and specific inhibitor of the vacuolar H^+-ATPase (V-ATPase), binding to the V_0 membrane domain of this eukaryotic acid pump. Although binding is known to involve the 16 kDa proteolipid subunit, contributions from other V_0 subunits are possible that could account for the apparently different inhibitor sensitivities of pump isoforms in vertebrate cells. In this study, we used a fluorescence quenching assay to directly examine the roles of V_0 subunits in inhibitor binding. Pyrene-labeled V_0 domains were affinity purified from *Saccharomyces* vacuolar membranes, and the 16 kDa proteolipid was subsequently extracted into chloroform and methanol and purified by size exclusion chromatography. Fluorescence from the isolated proteins was strongly quenched by nanomolar concentrations of both concanamycin and an indolyl pentadieneamide compound, indicating high-affinity binding of both natural macrolide and synthetic inhibitors. Competition studies showed that these inhibitors bind to overlapping sites on the proteolipid. Significantly, the 16 kDa proteolipid in isolation was able to bind inhibitors as strongly as V_0 did. In contrast, proteolipids carrying mutations that confer resistance to both inhibitors showed no binding. We conclude that the extracted 16 kDa proteolipid retains sufficient fold to form a high-affinity inhibitor binding site for both natural and synthetic V-ATPase inhibitors and that the proteolipid contains the major proportion of the structural determinants for inhibitor binding. The role of membrane domain subunit a in concanamycin binding and therefore in defining the inhibitor binding properties of tissue-specific V-ATPases is critically re-assessed in light of these data.

The vacuolar H^+-ATPase (V-ATPase)[1] is a multisubunit membrane protein found in virtually all eukaryotic cells, where it couples the free energy of ATP hydrolysis to proton pumping (*1*, *2*). Ion translocation occurs in the V_0 domain, an ~240 kDa integral membrane complex of five different subunits with a probable stoichiometry of $a_1d_1c_4c'_1c''_1$ (*3*). In common with the F_1F_0-ATPase, the mechanism of the V-ATPase involves generation of rotational motion in the soluble, ATP-hydrolyzing V_1 domain that is transmitted to a multimeric subunit c/c′/c″ "rotor" in V_0 via a central stalk structure (*4*−*6*). A second, peripheral stalk fixes membrane subunit a with respect to V_1, allowing movement of the c/c′/c″ rotor subunits relative to subunit a. All of these membrane subunits contain residues directly involved in proton translocation (*7*−*9*), and the dynamic interface between the c and a subunits has been proposed as the site of proton translocation (*10*−*12*).

Physiological roles of the V-ATPase include acidification of endosomal and lysosomal compartments (*2*), and in some cell types, the pump is responsible for proton extrusion across the plasma membrane. This acid secretion function has led to considerable interest in developing inhibitors as potential therapeutics (*13*−*16*). Attempts to develop V-ATPase-targeted drugs have focused on the naturally occurring macrolide antibiotics concanamycin and bafilomycin, highly specific inhibitors of the V-ATPase at nanomolar concentrations (*17*, *18*) reported to bind to the V_0 membrane domain of the pump. Derivatives of these macrolides (*14*, *18*, *19*) and small molecules based on the presumptive pharmacophore (*16*, *20*) are also potent V-ATPase inhibitors and exhibit tissue selectivity (*14*, *16*, *19*, *20*). In vertebrates, this apparently selective inhibition of ATPases from particular cell types has been correlated with the differential expression of up to four isoforms of subunit a. In contrast, only one form of subunit c appears to be expressed in vertebrate cells. The proposition is therefore that V-ATPases incorporating different subunit a isoforms exhibit different inhibitor binding properties, resulting in different degrees of sensitivity and

† This work was supported by grants from the European Union Framework V (QLRT-1999-31801) and UK BBSRC (24/b14097).

* To whom correspondence should be addressed: Research Institute of Membrane and Systems Biology, LIGHT Laboratories, Faculty of Biological Sciences, University of Leeds, Woodhouse Lane, Leeds LS2 9JT, U.K. Telephone: (+44) 113 3437766. Fax: (+44) 113 3433167. E-mail: m.a.harrison@leeds.ac.uk.

‡ School of Biochemistry and Microbiology, University of Leeds.

§ School of Chemistry, University of Leeds.

|| Glasgow Caledonian University.

[1] Abbreviations: DDM, *n*-dodecyl β-D-maltoside; SB-242784, (2*Z*,4*E*)-5-(5,6-dichloro-2-indolyl)-2-methoxy-*N*-(1,2,2,6,6-pentamethylpiperidin-4-yl)-2,4-pentadienamide; PCD, *N*-(1-pyrenyl)cyclohexylcarbodiimide; PM, *N*-(1-pyrenyl)maleimide; V-ATPase, vacuolar H^+-translocating ATPase.

10.1021/bi051529h CCC: $30.25 © 2005 American Chemical Society
Published on Web 10/21/2005

the apparent tissue selectivity. This has largely been the premise on which the development of V-ATPase-targeted drugs has been based. Early studies suggested that subunit a is the macrolide inhibitor binding site (*21*, *22*). However, a number of other studies have indicated that subunit c is the primary bafilomycin-binding component in V_0 (*23*−*25*). None of these studies was able to show whether the bafilomycin binding site is exclusively located on subunit c, and the question regarding the molecular basis for differential sensitivity of cellular V-ATPase activities remains unanswered. In this study, we have used a fluorescence quenching assay to examine directly the binding of both natural and synthetic V-ATPase inhibitors to purified subunit c and V_0 membrane domain from *Saccharomyces*. These studies show categorically that inhibitors can bind specifically to the subunit c component with high affinity, and that this binding can occur even in the absence of other subunits of the V_0 membrane domain. This study therefore raises questions about the role of subunit a in defining the inhibitor binding properties of the V-ATPase.

EXPERIMENTAL PROCEDURES

Plasmid Construction, Mutagenesis, and Yeast Strains. Preparation of plasmid constructs for wild-type, cysteine-depleted, and single-cysteine mutant forms of the *Nephrops* 16 kDa proteolipid and their subsequent expression have been described previously (*26*). A cDNA encoding a form of the *Saccharomyces cerevisiae* subunit a homologue Vph1p without cysteine residues was constructed by QuikChange mutagenesis (Promega) using wild-type *VPH1* modified to encode an N-terminal hexahistidine tag [MRGS$(H)_6$] with pSK-Bluescript (Stratagene) as a template. The native cysteine residues were replaced with amino acids that multiple-sequence alignments suggest are most likely to be tolerated substitutions at each location (see the Supporting Information). Mutations were confirmed by DNA sequencing. Engineering and constitutive expression of Vma3p polypeptides with C-terminal hemagglutinin (HA) epitope and bafilomycin resistance-conferring mutations have been described previously (*27*).

A haploid *S. cerevisiae* strain carrying disruptions in both the *VMA3* and *VPH1* genes was constructed from a haploid *vma3* strain (*MAT*α, *vma3*::*LEU2*, *trp1*, *ura3*, *his3*, *ade2*) by transformation with a linearized cDNA construct comprising the *VPH1* coding region disrupted by insertion of a 1156 bp *HIS3* gene cassette at an *Eco*RI site within the *VPH1* cDNA. Integration of this construct at the chromosomal *VPH1* locus was confirmed by generation of a 1.63 kb *HIS3* PCR product using a primer pair of V1 (5′-GCACAACAATTAATTTCCGCG-3′) and V2 (5′-TTAGCTTGAAGCGGAAGAGCC-3′). These primers anneal to sites within *VPH1* that flank the *Eco*RI site and which are separated by 480 bp of sequence. Genomic DNA isolated from His^+ transformants was used as a template for the PCRs.

Simultaneous coexpression of *Nephrops* 16 kDa proteolipid and Vph1p mutants was achieved by subcloning cDNAs for both into the yeast expression vector pESC-URA (Stratagene) that contains dual galactose-inducible *GAL1* and *GAL10* promoters and a *URA3* selectable marker. *VPH1* cDNAs were purified as *Hin*dIII−*Xba*I fragments and subcloned between the *Hin*dIII and *Nhe*I sites downstream from the *GAL1* promoter. *Not*I and *Sac*I restriction sites in the multiple-cloning site downstream of the *GAL10* promoter were modified by QuikChange mutagenesis to give *Sac*I and *Xho*I sites, respectively, compatible with the restricted ends of the *Nephrops* proteolipid cDNAs. The pESC-URA constructs were used to transform a haploid *S. cerevisiae* strain carrying disruptions in both the *VMA3* and *VPH1* genes (*MAT*α, *vma3*::*LEU2*, *vph1*::*HIS3*, *trp1*, *ura3*, *ade2*; see the Supporting Information), using the lithium acetate procedure (*28*). Transformants that were no longer auxotrophic for uracil were screened for complementation of the conditional lethal phenotype associated with *vma* mutations by testing for growth on yeast extract-peptone medium buffered with 50 mM MOPS and 50 mM MES and titrated to pH 7.5 with NaOH. Media were supplemented with 1% galactose and 1% raffinose. For mutants that were unable to support growth at pH 7.5, cells were grown on synthetic minimal medium [0.67% yeast nitrogen base, 30 μg/mL tryptophan, 20 μg/mL adenine, and 50 mM MOPS/MES-NaOH (pH 5.5), with 1% galactose and 1% raffinose].

Membrane Isolation and Purification of Labeled Proteins. Vacuolar membrane vesicles were prepared as described in ref *29*. ATPase activity was determined colorimetrically as detailed in ref *30*. Concanamycin A (Fluka) and SB-242784 were added from stock solutions in DMSO such that the level of solvent never exceded 0.5% of the total volume. Synthesis of 5-(5,6-dichloro-2-indolyl)-2-methoxy-*N*-(1,2,2,6,6-pentamethylpiperidin-4-yl)-2,4-pentadienamide (SB-242784) is described in ref *16*. Labeling with *N*-(1-pyrenyl)maleimide (PM) or *N*-(1-pyrenyl)cyclohexylcarbodiimide (PCD) was performed as described in ref *31*. After solubilization in *n*-dodecyl β-D-maltoside (DDM), V_0 domains were affinity purified as described in ref *31*. Extraction of subunit c polypeptides into a chloroform/methanol mixture was performed as described in ref *26*. Solvent was removed by drying under vacuum, and the extracted polypeptides were redissolved in 50 mM HEPES-NaOH and 0.1 mM EDTA (pH 7.6) supplemented with 0.1% DDM. The solubilized proteolipid was further purified by size exclusion chromatography through a Superdex 200 HR column (Pharmacia Biotech, Little Chalfont, U.K.) in the same buffer. Fractions were screened for pyrene fluorescence, pooled, and analyzed for the presence of the proteolipid by SDS−PAGE and immunoblotting.

Fluorescence Spectroscopy. Measurement of fluorescence from the labeled proteins in the presence of varying concentrations of inhibitor (I) gave nonlinear plots of F_0/F versus inhibitor concentration, where F_0 and F are the fluorescence yield in the absence and presence of inhibitor, respectively. Measurements were made in a Varian Cary Eclipse fluorescence spectrometer at 20 °C, with excitation of pyrene fluorescence at 342 nm. Fluorescence emission spectra were recorded in the range of 350−500 nm. Slit widths were set at 5 nm. Dissociation constants (K_d) for each inhibitor were determined by fitting curves to plots of $(F_0 - F)/F_0$ (% quenching) versus inhibitor concentration according to the quadratic binding equations of Parikh et al. (*32*):

$$\%\ \text{quenching} = C_1\left(\frac{S - \sqrt{S^2 - 4I_T P_T}}{2}\right) - C_2 I_T$$

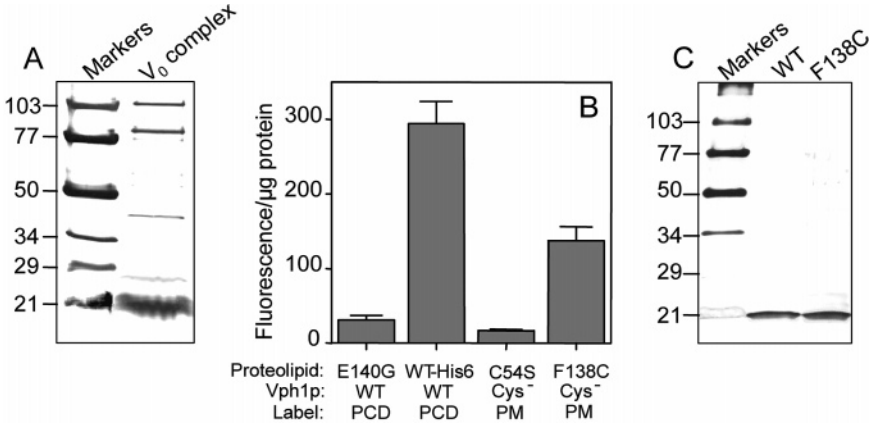

FIGURE 1: Purification of V_0 complexes and 16 kDa proteolipids. (A) V_0 complexes incorporating His_6-tagged subunits were affinity purified on Ni^{2+}−NTA agarose after solubilization of vacuolar membranes with DDM and analyzed by SDS−PAGE and silver staining. The example shown is for His_6-tagged *Nephrops* proteolipid copurified with wild-type Vph1p. (B) Specificity of pyrene labeling in V_0. Fluorescence emission from affinity-purified V_0 containing the specified combinations of Vph1p and proteolipid is expressed as a function of protein concentration. Values are means (±standard deviation) of three determinations. (C) SDS−PAGE of His_6-tagged wild-type (WT) and C54S/F138C double mutant (F138C) *Nephrops* proteolipids. The polypeptides were extracted from affinity-purified V_0 complexes with a chloroform/methanol mixture, and further purified by size exclusion chromatography after recovery into detergent solution. The gel was stained with silver.

where $S = I_T + P_T + K_d$, where I_T is the total inhibitor concentration, and P_T is the concentration of fluorescently labeled protein. C_1 and C_2 are constants related to the fluorescence components arising from the labeled protein, free inhibitor, and bound inhibitor (*32*). Curve fitting using the nonlinear fitting tool within Origin 7 (OriginLab, Northampton, MA) was used to determine the parameters C_1, C_2, and K_d for an experimentally controlled value of P_T. C_2 is negligible because of the low fluorescence arising from the inhibitor molecule.

The protein assay using the CBQCA [3-(4-carboxybenzyloyl)quinoline-2-carboxaldehyde] dye binding method was performed as described in ref *26*. The concentration of pyrene dye was determined from the absorbance at 340 nm assuming an extinction coefficient at that wavelength of 40 000 M^{-1} cm^{-1}. SDS−PAGE and immunoblotting were performed as described in ref *26*.

RESULTS

Site-Directed Labeling of the 16 kDa Proteolipid. The 16 kDa proteolipid folds as a bundle of four transmembrane helices, and mutations in helix 4 can confer resistance to bafilomycin (*33*). This helix also has sites accessible from the lipid phase of the membrane (*31*), which is the presumed route by which lipophilic inhibitors access the V-ATPase. We therefore selected residues in this region as targets for labeling with thiol- and carboxyl-reactive fluorescent probes, the aim being to provide sites that could report on inhibitor binding, detected in the form of inhibitor-dependent changes in fluorescence. The yeast Vma3p proteolipid is not amenable to cysteine replacement mutagenesis, becoming nonfunctional when its native cysteine residues are mutated (*12*). To compensate for this problem, we used the *Nephrops* proteolipid as a Vma3p surrogate since it substitutes for Vma3p (*30*) and supports full assembly and activity of the V-ATPase. Phe^{138} on helix 4 of the *Nephrops* proteolipid was targeted for labeling with PM by introduction of a unique cysteine residue at this site in a cysteine-less C54S mutant template, giving the mutant n-F138C. To maximize specificity of PM labeling, this proteolipid mutant was coexpressed in a *υma3*/*υph1* double knockout yeast strain with a cysteine-depleted Vph1p polypeptide (v-Cys^-) carrying an N-terminal six-His tag. As a control for labeling specificity, the cysteine-depleted Vph1p was also coexpressed with the cysteine-depleted, but fully functional, C54S mutant form of the proteolipid (n-C54S) (*30*). The carbodiimide reagent PCD also gives highly specific labeling of the proteolipid via modification of the protonated glutamate residue on helix 4 (*31*), which we exploited to provide a second labeling site. For this labeling strategy, His6-tagged wild-type *Nephrops* proteolipid was expressed in a yeast strain disrupted for the *VMA3* gene encoding the native proteolipid, and labeled at Glu^{140}. To provide negative controls for inhibitor binding, we also expressed bafilomycin-resistant mutant and wild-type forms of the native yeast Vma3p proteolipid and labeled these with PCD at the corresponding helix 4 glutamate (Glu^{137}) before purification.

Vacuolar membranes were isolated from yeast strains transformed with each expression construct and reacted with the appropriate pyrenyl probe. Fluorescently labeled V_0 domains were then isolated by Ni^{2+}−NTA affinity chromatography. In the case of V_0 labeled at Glu^{140} with PCD, purification was mediated via a C-terminal six-His tag on the *Nephrops* proteolipid (*34*). Membrane domains incorporating coexpressed Vph1p and proteolipid were isolated via the six-His tag at the N-terminus of Vph1p. In either case, fractions highly enriched in V_0 were recovered (Figure 1A). The affinity-purified V_0 fraction contains polypeptides migrating with apparent masses of 20, 42, and 110 kDa corresponding to the proteolipid, Vma6p, and Vph1p subunits, respectively. A band migrating at approximately 26 kDa could be the Vma16p (subunit c″) polypeptide or the anomalously migrating dimer of the *Nephrops* proteolipid. A polypeptide migrating with an approximate mass of 80 kDa is a degradation product of Vph1p that is also recognized by monoclonal antibodies to that subunit (data not shown). Isolated V_0 complexes were fluorescent irrespective of the site of fluorophore attachment, although PCD modification of Glu^{140} was more efficient than PM labeling (Figure 1B). Relatively low levels of PCD labeling were detected for V_0

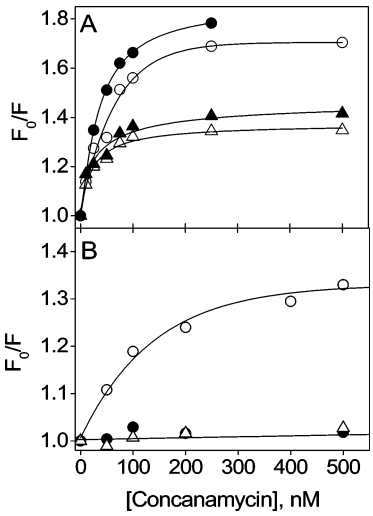

FIGURE 2: Concanamycin-dependent quenching of fluorescence from pyrene-labeled 16 kDa proteolipids. (A) Variable fluorescence F was measured for affinity-purified, pyrene labeled V_0 complexes (15 μg/mL) (○ and △) and isolated *Nephrops* proteolipid (12−15 μg/mL) (● and ▲) in the presence of varying concentrations of concanamycin. V_0 and proteolipids were isolated from cells coexpressing His_6-tagged wild-type *Nephrops* proteolipid/wild-type Vph1p (labeled with PCD, circles) and n-F138C proteolipid/v-Cys^- Vph1p (labeled with PM, triangles). Fluorescence emission at 390 nm is expressed as a proportion of the fluorescence yield in the absence of inhibitor (F_0). (B) Concanamycin-dependent fluorescence quenching measured as in panel A for HA-tagged Vma3p proteolipids (12−14 μg/mL) labeled at Glu^{137} with PCD: wild type (○) and mutants Y142H (●) and Y142H/F135L (△). All data points are the means of three individual experiments.

containing a control Glu^{140} → Gly *Nephrops* proteolipid mutant (E140G, Figure 1B), with the residual fluorescence due possibly to labeling of the subunit c′ and subunit c″ proteolipids. V_0 complexes containing the cysteine-depleted forms of proteolipid and Vph1p exhibited little fluorescence after reaction with PM (Figure 1B). Proteolipids were subsequently purified by extracting the V_0 preparations with chloroform/methanol. After the solvent had been removed and the proteolipids had been redissolved in buffer containing DDM, they were further separated by size exclusion chromatography, the fluorescent protein eluting as a single species with an apparent mass of 65 kDa (data not shown). Analysis by SDS−PAGE showed the extracted proteins to be highly purified (Figure 1C). The stoichiometry of pyrene labeling, estimated from the proteolipid concentration and the pyrene absorbance at 340 nm, was found to be 0.22 and 0.16 pyrene/proteolipid for the PCD-labeled wild-type and PM-labeled n-F138C polypeptides, respectively. The n-C54S proteolipid was completely nonfluorescent. We are therefore able to conclude that, for both pyrene probes, reasonable levels of labeling have been achieved with a high degree of specificity for the target residue. Similar levels of purification and fluorescence yield were obtained for wild-type and bafilomycin-resistant mutant forms of the native yeast Vma3p proteolipid, labeled with PCD (data not shown).

Direct Quenching of Fluorescence from Site-Specific Pyrene Labels by Concanamycin A. Fluorescence from pyrene conjugated to V_0 proteins showed significant nonlinear quenching when titrated with sub-micromolar concentrations of concanamycin (Figure 2). For V_0 complexes, this quenching was partly dependent on the location of the pyrene adduct, occurring with greater efficiency when the fluorophore was attached to Glu^{140} of the proteolipid than when attached to the cysteine of the F138C mutant (Figure 2A). However, for each labeling site, similar levels of quenching were obtained with purified proteolipids or V_0 domains (Figure 2A), indicating that concanamycin can bind to the homogeneous polypeptide or to the multiprotein membrane domain with equal efficiency. The nonlinear character of the plots of F_0/F versus concanamycin concentration is consistent with high-affinity binding of the quenching species to the fluorescent protein and precludes simple collisional quenching. Furthermore, it is inconsistent with any significant contribution from static quenching at higher inhibitor concentrations, since this would tend to give upward-curving plots (see ref *35* for a discussion of this topic). In control experiments, fluorescence from free pyrene dye in detergent solution was unaffected by addition of inhibitor (data not shown). From these data, we conclude that the isolated proteolipid in detergent solution can bind concanamycin and that this binding directly results in fluorescence quenching from the pyrene adducts attached to the protein.

To exclude the possibility that quenching results from a simple, nonspecific association between lipophilic inhibitor compound and the hydrophobic 16 kDa proteolipid, we used the fluorescence quenching assay to test binding to forms of the native yeast Vma3p proteolipid carrying mutations that confer resistance to both bafilomycin and indolyl pentadieneamide inhibitors (*27*). Purified Vma3p proteolipids carrying Tyr^{142} → His or Tyr^{142} → His/Phe^{135} → Leu mutations, labeled with PCD at the conserved helix 4 glutamate residue (Glu^{137}) and purified as in Figure 1, showed no quenching with concanamycin (Figure 2B). In contrast, fluorescence from the wild-type Vma3p labeled with PCD was strongly quenched by the macrolide (Figure 2B). These data clearly indicate that concanamycin is unable to bind to the mutant Vma3p polypeptides, but that the isolated wild-type yeast polypeptide retains a high-affinity concanamycin binding site.

Concanamycin has a weaker overall effect on the fluorescence from samples containing the F138C mutant proteolipid than it does on the wild-type protein (Figure 2A), reflected as lower F_0/F values for the mutant at any given inhibitor concentration. Sequence alignments indicate that residue Phe^{138} of the *Nephrops* proteolipid is equivalent to Phe^{135} of Vma3p, a site at which changes in amino acid side chains can have profound effects on inhibitor binding, manifested in vivo as resistance (*25*). It might therefore be expected that addition of a pyrene group to this site would also prevent inhibitor binding. This would have the effect of decreasing the overall quenching effect of concanamycin, consistent with the data in Figure 2A. However, fluorescence from the pyrene attached to the mutant proteolipid is still quenched by the inhibitor, clearly indicating that the fluorescent group attached to the F138C site does still report inhibitor binding. We can interpret this quenching in either of two ways. (1) The pyrene group attached to the F138C mutant proteolipid does not prevent inhibitor binding, but F_0/F ratios are lower because the quenching photochemistry is less efficient than it is for the couple formed between inhibitor and PCD-labeled wild-type protein. This is as much a function of the relative geometry of the fluorophore and quencher as it is a simple indicator of differences in their

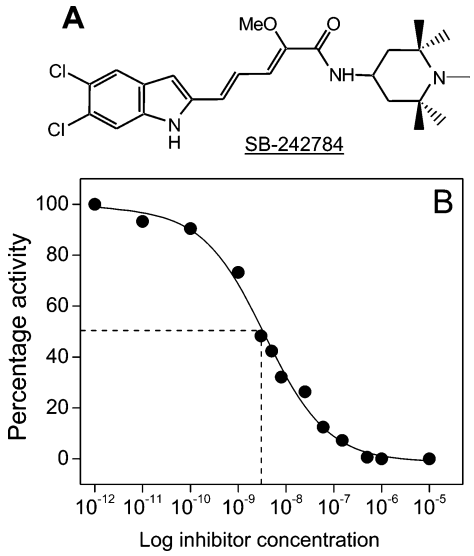

FIGURE 3: SB-242784 is a potent inhibitor of the *Saccharomyces* V-ATPase. (A) The spacing and geometry of critical functional groups in the macrolide ring of concanamycin A are mimicked by those of SB-242784. (B) V-ATPase was isolated from wild-type yeast cells by glycerol gradient centrifugation after solubilization of vacuolar membranes in DDM. Rates of release of inorganic phosphate from MgATP are expressed relative to the maximal rate in the absence of inhibitor [2.3 μmol of phosphate (mg of protein)$^{-1}$ min^{-1}].

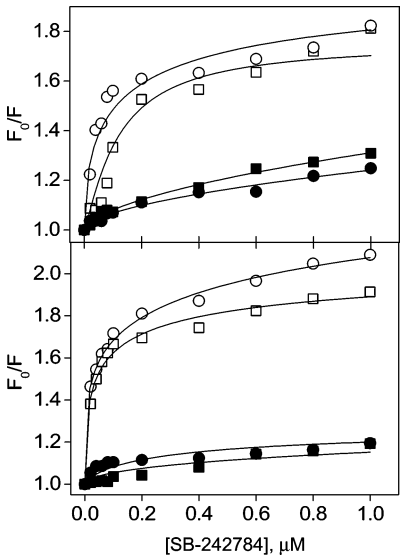

FIGURE 4: Quenching of fluorescence from purified V_0 and 16 kDa proteolipids indicates SB-242784 binding. (A) Variable fluorescence was measured for affinity-purified, pyrene-labeled V_0 complexes (15 μg/mL) in the presence of varying concentrations of SB-242784. V_0 was isolated from cells coexpressing His_6-tagged wild-type *Nephrops* proteolipid with wild-type Vph1p (PCD-labeled, circles), and from cells coexpressing the n-F138C proteolipid with the v-Cys$^-$ cysteine-less Vph1p (PM-labeled, squares). Fluorescence emission (F) at 390 nm is expressed as a proportion of the fluorescence yield in the absence of SB-242784 (F_0). The purified proteins were preincubated with (filled symbols) or without (empty symbols) 100 nM concanamycin. (B) Fluorescence quenching measured as in panel A, with isolated PCD-labeled wild-type (circles) and PM-labeled n-F138C (squares) *Nephrops* 16 kDa proteolipids (12−15 μg/mL). Data points are the means of three individual experiments.

distance apart. (2) Alternatively, even though a labeled F138C proteolipid might not itself be capable of binding an inhibitor molecule, quenching could still occur if it was associated with an unlabeled polypeptide that was able to bind an inhibitor. However, this second explanation requires that the purified proteolipid used in this study be to some degree multimeric, and although size exclusion chromatography does suggest a mass of the isolated proteolipid of 65 kDa, this will also include a DDM micelle that could contribute as much as 50 kDa to the overall mass (*36*). The inherent inaccuracy of the chromatographic mass determination therefore makes it impossible to discriminate with any confidence between the monomer and dimer, and further work is needed to resolve this issue.

SB-242784 Is a Potent Inhibitor of the Saccharomyces V-ATPase. The chemical moieties that confer the activity of the macrolide V-ATPase inhibitors are reported to include the hemiketyl group, and hydroxy and vinylic methoxy groups optimally spaced by the dienic system of the macrolide ring (*37*). Indolyl pentadieneamide compounds such as SB-242784 mimic this arrangement (Figure 3A), with the molecule carrying functional groups analogous to those found in the macrolides, spaced according to the same basic geometry (*16*). Since these compounds are also reported to be specific and potent inhibitors of mammalian V-ATPases (*16*, *20*), SB-242784 can be considered to represent a form of minimal inhibitor unit. By establishing whether this small molecule inhibitor can also bind directly to the V-ATPase membrane domain components, we can indirectly examine the contributions to binding made by specific structural elements contained within the macrolide molecules. SB-242784 also contains an indolyl group that has spectral properties that make it particularly suitable for forming energy transfer couples with pyrene fluorophores. Consequently, quenching of fluorescence from the proteolipid-linked pyrene can provide a direct assay of binding of SB-242784 to the V-ATPase. However, we first needed to establish that SB-242784 is also a potent inhibitor of the *Saccharomyces* V-ATPase. The effect of SB-242784 on the activity of the isolated yeast enzyme was determined from the concentration-dependent inhibition of release of inorganic phosphate from MgATP (Figure 3B). SB-242784 inhibited the fungal enzyme with an apparent IC_{50} of 3.5 $\pm$ 1 nM (Figure 3B), lower than the value of 80 nM reported for its inhibition of the chicken osteoclast V-ATPase (*16*).

SB-242784 Quenching of Pyrene Fluorescence Indicates Direct Binding to the 16 kDa Proteolipid. SB-242784 was also an efficient quencher of fluorescence from pyrene adducts on the 16 kDa proteolipid (Figure 4). As with concanamycin, the nonlinear plots of F_0/F as a function of SB-242784 concentration indicate binding of the quencher species to the fluorescent protein. The efficiency of quenching by SB-242784 was not dependent on the site of pyrene labeling (Figure 4A), and was not significantly different when measured with preparations of V_0 (Figure 4A) or isolated 16 kDa proteolipid (Figure 4B). From this, we conclude that the small molecule inhibitor can bind directly to the proteolipid component of the V-ATPase membrane domain and that this binding can occur even in the absence of other V-ATPase subunits. Furthermore, SB-242784 and concanamycin A appear to compete for the same binding site on the proteolipid, since preincubation with the macrolide abolished the ability of SB-242784 to quench pyrene fluorescence from either isolated V_0 (Figure 4A) or purified proteolipid (Figure 4B). Concanamycin and SB-242784 binding sites must

Table 1: Fluorometrically Determined Dissociation Constants for Binding of the Inhibitor to V_0 and Proteolipid[a]

	SB-242784			concanamycin		
labeled protein	K_d (nM)	χ^2/DoF	R^2	K_d (nM)	χ^2/DoF	R^2
n-WT-His_6 proteolipid	7.7 ± 2.3	0.35	0.99	17.8 ± 2.5	0.81	0.99
n-F138C proteolipid	8.5 ± 4.2	0.82	0.99	13.7 ± 13.0	3.89	0.97
V_0 (n-WT-His_6)	4.6 ± 2.2	5.74	0.98	24.3 ± 9.0	5.31	0.98
V_0 (n-F138C/v-Cys^-)	6.2 ± 3.0	1.18	0.98	15.7 ± 13.3	1.19	0.99

[a] Parameters were derived by fitting curves to the fluorescence quenching data according to the binding equation described in Experimental Procedures. K_d values are expressed $\pm$ the standard error of the mean ($n = 3$). The reduced χ^2 (χ^2/DoF) and correlation coefficient (R^2) provide a measure of the quality of the fit of the experimental data to the binding model. The n-F138C proteolipid is the C54S/F138C double mutant polypeptide containing only a single engineered cysteine residue, and v-Cys^- is the cysteine-less Vph1p polypeptide.

overlap structurally to some extent, and the potency of SB-242784 as a V-ATPase inhibitor therefore stems from its ability to bind at this shared site. Experiments with PCD-labeled NtpK, the 16 kDa proteolipid of the Na^+-translocating V-ATPase from *Enterococcus*, revealed no fluorescence quenching by inhibitors (data not shown). This prokaryotic V-ATPase is reported to be insensitive to the macrolide antibiotics (*38*).

Treatment of the fluorescence quenching data according to the quadratic binding equations in ref *32* allows estimation of the dissociation constant K_d without direct determination of the concentration of the protein−inhibitor complex (Table 1). Apparent dissociation constants for SB-242784 were in the range from 4.6 ± 2.3 to 8.5 ± 4.2 nM, values consistent with the observed IC_{50} for the compound in ATPase assays (Figure 3B). Similar estimations of K_d for concanamycin binding gave values in the range of 13.7−24.3 nM (Table 1). These values are 1−2 orders of magnitude higher than published IC_{50} values (*17*, *18*). Possible reasons for this discrepancy are discussed below. For each inhibitor, comparison of the estimated K_d values for binding to V_0 with those for binding to purified 16 kDa proteolipids revealed no significant difference (Table 1).

DISCUSSION

The key finding of this work is that the purified 16 kDa proteolipid can bind either complex or "mimimal" V-ATPase inhibitors with high affinity at sites that structurally overlap. Crucially, fluorimetrically determined K_d values for each inhibitor were not significantly different irrespective of whether they were measured with complete V_0 or with purified proteolipid. Binding of either inhibitor can therefore occur in the absence of any other V_0 subunit, and the proteolipid component of the membrane domain must therefore contain a major proportion of the structural determinants of the inhibitor binding site in the V-ATPase. Since an unfolded protein is highly unlikely to be competent for ligand binding, we also conclude that the 16 -kDa proteolipid must retain secondary or tertiary structure even after extraction into chloroform/methanol/water mixtures and recovery into detergent solution. Such a situation does exist with the related 8 kDa subunit c proteolipid from F_1F_0-ATPase that retains its helical hairpin fold in organic solvent as determined by solution state NMR (*39*).

For the synthetic inhibitor SB-242784, the fluorimetrically estimated K_d values (4.6−8.5 nM) are broadly consistent with the enzymologically determined IC_{50} (3.5 nM), suggesting that binding to either purified proteolipid or V_0 occurs with the same affinity as to the active enzyme. It is much less certain that this is also true of concanamycin, given the discrepancy between the estimated K_d and published IC_{50} values. There are several possible explanations for this discrepancy. Binding of concanamycin with an affinity comparable to the reported IC_{50} values might require a specific structural component (either polypeptide or lipid) or conformation that has been lost during purification of the V_0 complex. It is certainly the case that V_0 dissociated from V_1 is impermeable to protons (*21*, *22*), implying some change in conformation to a "closed" state after removal of the soluble domain. However, the most straightforward explanation for the anomalously high K_d for concanamycin is that the macrolide has undergone significant decomposition during the course of the experiments. Both concanamycin and bafilomycin are reported to be extremely labile (*40*), whereas SB-242784 is relatively stable. Whatever the explanation for this discrepancy, it is important to stress that none of them relates to binding of the minimal synthetic inhibitor SB-242784 since the estimated K_d for binding to isolated proteolipid or to V_0 is essentially the same as the IC_{50} of the compound. Furthermore, the close similarity between K_ds for binding to either proteolipid or V_0 implies that the additional subunits found in the membrane domain have no influence on inhibitor binding.

Our data can therefore be interpreted as meaning that subunit a does not contribute to the inhibitor binding site, placing a question mark against its proposed role in defining the relative selectivity of V-ATPase inhibitors. However, several factors mitigate against the exclusion of a role for subunit a. First, we do not see any binding of inhibitors to the isolated Vma3p polypeptides carrying mutations conferring resistance to bafilomycin even though binding with low micromolar affinity does still occur in vivo (*25*, *33*), implying that an additional component found in the intact V-ATPase also contributes to binding. Second, the fluorometrically determined K_d value for binding to the V_0 domain is actually the average value for what are likely to be multiple binding sites on each individual protein complex. Because of the limitations in the precision of the experimental method, an interaction between subunit a and any one of these multiple binding sites in V_0 could influence inhibitor binding to some extent without being detected as a difference in the overall K_d compared to that determined for the proteolipid alone. Finally, and related to the point about subunit conformation in V_0 discussed above, our experimental method does not allow us to eliminate the possibility that conformational changes occurring as a result of V_0 isolation alter or destroy a binding site to which subunit a contributes in the native enzyme.

A counter to this argument is that comprehensive screening has failed to identify any bafilomycin resistance mutations in the fungal subunit a homologue, providing indirect evidence that this V_0 subunit does not contribute to the inhibitor binding site (*25*). If subunit a is not directly involved in inhibitor binding, what factors might explain the apparent selectivity of inhibitors for different V-ATPase isoforms in vertebrates? One possibility is that natural variations in membrane lipid composition, and therefore in the physical properties of the membrane, influence partitioning of inhibi-

tors into the bilayer. Variations in partitioning effects between specific membranes could be reflected as differences in apparent IC_{50} values for a particular inhibitor. Although this may not wholly account for the up to 25-fold variations in IC_{50} measured for V-ATPases in different cells with the same inhibitor (*14*, *16*, *20*), it is consistent with the observation that apparent IC_{50} values for V-ATPase inhibitors vary with the concentration of membranes included in the assay (*17*).

Bafilomycin A1 and concanamycin A have dimensions of approximately 17 and 24 Å, respectively, along their long axes, with some 12 Å spacing between the hydroxyl and hemiketyl groups. In yeast, bafilomycin resistance mutations span a 13-residue region equivalent to a vertical distance of approximately 20 Å (*33*). A macrolide antibiotic molecule can therefore overlap these positions only if it is fully extended and oriented with its major axis parallel to that of the transmembrane helix. Mutations at positions 135 and 142 in helix 4 of the Vma3p proteolipid also confer resistance to SB-242784 (*27*), and this molecule can span the ≈10.5 Å between these residues if it adopts the same orientation as the macrolide when bound. From this, we conclude that the mechanism of action of both natural and synthetic inhibitors requires them to bind to helix 4 of the proteolipid, and when bound, their long axes must be oriented parallel to that of the helix. Furthermore, our data suggest that the region of the macrolide ring mimicked by SB-242784 is the key structure that facilitates binding of concanamycin to this helix of the proteolipid.

Recent work on characterization of fungal mutants exhibiting resistance to bafilomycin and concanamycin found the resistance-conferring mutations to be clustered primarily on helices 2 and 4 of the proteolipid (*25*, *33*). According to the recently published structure of the NtpK rotor complex (*41*), the 16 kDa proteolipid complex is a decameric ring of four helix bundles, with alternating helix 1−helix 3 units forming an inner ring and alternating helix 2−helix 4 units forming an outer ring that interfaces with the lipid phase. By homology, bafilomycin resistance mutations within the eukaryotic proteolipid will be clustered at the intermolecular helix 2−helix 4 interface (*33*) and the binding site for the macrolide antibiotics may therefore require structural contributions from both partners in a dimeric proteolipid unit. However, as discussed above, in this study we have not been able to unambiguously resolve the aggregation state of the purified proteolipid, and the organization of the inhibitor binding site associated with this purified protein remains uncertain.

Why does binding of the inhibitor to the 16 kDa proteolipid result in inhibition of the V-ATPase? Bowman and coworkers have proposed that intercalation of the inhibitor between transmembrane helices in the proteolipid complex could physically obstruct its rotation relative to subunit a (*33*). According to current functional models, this rotationally driven but transient interaction between proteolipid and subunit a is a crucial part of the proton translocation mechanism (*2*, *10*−*12*). For this mechanism to work, inhibitor binding would need to resist the relatively large mechanical force generated by the rotational mechanism of the V-ATPase [≈40 pN for a rotor with a radius of 1 nm (*42*)], which is plausible. The corollary of this proposed mechanism is that occupation of only a single inhibitor binding site on the rotating proteolipid ring structure should ultimately be sufficient to bring about complete inhibition, occurring when the inhibitor-bound proteolipid rotates into a position adjacent to subunit a. This is supported by the observation that bafilomycin at a molar ratio of 1:1 with isolated V_0 is sufficient to completely inhibit acid-induced passive proton flow through the membrane complex (*22*). Intercalation of the inhibitor between transmembrane helices could also disrupt packing within the membrane domain, or prevent conformational changes from occurring that could be part of the protonation−deprotonation mechanism (*43*). Analysis by ESR of the interaction between V-ATPase inhibitors and the *Nephrops* 16 kDa proteolipid has shown that inhibitor binding occurs at the protein−lipid interface and that binding causes increased immobilization of lipid molecules at the protein−membrane boundary (*44*). Immobilized lipid would also be expected to interfere with the rotational mechanics of the V-ATPase.

Although the data presented in this study cast doubt on the involvement of subunit a in binding the bafilomycin family of inhibitors to the V-ATPase, this issue ultimately remains unresolved. As a consequence, questions about the structural basis for tissue selectivity of V-ATPase inhibitors are also still open. However, the fluorimetric assay described in this study represents a powerful and sensitive tool with which we can start to address these questions, with applications not only in inhibitor design but also in the elucidation of their mechanism of action.

ACKNOWLEDGMENT

We thank Dr. Marcus Hemminga and his team at Wageningen Agricultural University (Wageningen, The Netherlands) for discussions and advice and Prof. Nathan Nelson (University of Tel Aviv, Tel Aviv, Israel) and Dr. Morris Manolson (Hospital for Sick Children, Toronto, ON) for providing yeast strains and cDNA clones.

SUPPORTING INFORMATION AVAILABLE

Full experimental details relating to construction of the cysteine-depleted Vph1p and single-cysteine replacement forms of the 16 kDa proteolipid. This material is available free of charge via the Internet at http://pubs.acs.org.

REFERENCES

1. Stevens, T. H., and Forgac, M. (1997) Structure, function and regulation of the vacuolar H^+-ATPase, *Annu. Rev. Cell Dev. Biol. 13*, 779−808.
2. Nishi, T., and Forgac, M. (2002) The vacuolar H^+-ATPases: Nature's most versatile proton pumps, *Nat. Rev. Mol. Cell Biol. 3*, 94−103.
3. Forgac, M. (1999) Structure and properties of the vacuolar H^+-ATPases, *J. Biol. Chem. 274*, 12951−12954.
4. Imamura, H., Nakano, M., Noji, H., Muneyuki, E., Ohkuma, S., Yoshida, M., and Yokoyama, K. (2003) Evidence for rotation of V_1-ATPase, *Proc. Natl. Acad. Sci. U.S.A. 100*, 2312−2315.
5. Noji, H., Yasuda, R., Yoshida, M., and Kinosita, K. (1997) Direct observation of the rotation of F-1-ATPase, *Nature 386*, 299−302.
6. Yokoyama, K., Nakano, M., Imamura, H., Yoshida, M., and Tamakoshi, M. (2003) Rotation of the proteolipid ring in the V-ATPase, *J. Biol. Chem. 278*, 24255−24258.
7. Kawasaki-Nishi, S., Nishi, T., and Forgac, M. (2001) Arg-735 of the 100-kDa subunit a of the yeast V-ATPase is essential for proton translocation, *Proc. Natl. Acad. Sci. U.S.A. 98*, 12397−12402.
8. Noumi, T., Beltran, C., Nelson, H., and Nelson, N. (1991) Mutational analysis of the yeast vacuolar H^+-ATPase, *Proc. Natl. Acad. Sci. U.S.A. 88*, 1938−1942.

9. Powell, B., Graham, L. A., and Stevens, T. H. (2000) Molecular characterization of the yeast vacuolar H^+-ATPase proton pore, *J. Biol. Chem. 275*, 23654−23660.
10. Grabe, M., Wang, H., and Oster, G. (2000) The mechanochemistry of V-ATPase proton pumps, *Biophys. J. 78*, 2798−2813.
11. Harrison, M. A., Finbow, M. E., and Findlay, J. B. C. (1997) Postulate for the molecular mechanism of the vacuolar H^+-ATPase (hypothesis), *Mol. Membr. Biol. 14*, 1−3.
12. Kawasaki-Nishi, S., Nishi, T., and Forgac, M. (2003) Interacting helical surfaces of the transmembrane segments of subunits a and c′ of the yeast V-ATPase defined by disulfide-mediated cross-linking, *J. Biol. Chem. 278*, 41908−41913.
13. Farina, C., and Gagliardi, S. (1999) Selective inhibitors of vacuolar H^+-ATPase of osteoclasts with bone antiresorptive activity, *Expert Opin. Ther. Pat. 9*, 157−168.
14. Keeling, D. J., Herslof, M., Mattson, J. P., and Ryberg, B. (1998) Tissue-selective inhibition of vacuolar acid pumps, *Acta Physiol. Scand. 163*, 195−201.
15. Hall, T. J., and Schaueblin, M. (1994) A pharmacological assessment of the mammalian osteoclast vacuolar H^+-ATPase, *Bone Miner. 27*, 159−166.
16. Gagliardi, S., Nadler, G., Consolandi, E., Parini, C., Morvan, M., Legave, M. N., Belfiore, P., Zocchetti, A., Clarke, G. D., James, I., Nambi, P., Gowen, M., and Farina, C. (1998) 5-(5,6-Dichloro-2-indolyl)-2-methoxy-2,4-pentadienamides: Novel and selective inhibitors of the vacuolar H^+-ATPase of osteoclasts with bone antiresorptive activity, *J. Med. Chem. 41*, 1568−1573.
17. Bowman, E. J., Siebers, A., and Altendorf, K. (1988) Bafilomycins: A class of inhibitors of membrane ATPases from microorganisms, animal cells, and plant cells, *Proc. Natl. Acad. Sci. U.S.A. 85*, 7972−7976.
18. Drose, S., Bindseil, K. U., Bowman, E. J., Siebers, A., Zeeck, A., and Altendorf, K. (1993) Inhibitory effects of modified bafilomycins and concanamycins on P- and V-type adenosinetriphosphatases, *Biochemistry 32*, 3902−3906.
19. Gagliardi, S., Gatti, P. A., Belfiore, P., Zochetti, A., Clarke, G. D., and Farina, C. (1998) Synthesis and structure−activity relationships of bafilomycin A1 derivatives as inhibitors of vacuolar H^+-ATPase, *J. Med. Chem. 41*, 1883−1893.
20. Visentin, L., Dodds, R. A., Valente, M., Misiano, P., Bradbeer, J. N., Oneta, S., Liang, X. G., Gowen, M., and Farina, C. (2000) A selective inhibitor of the osteoclastic V-H^+-ATPase prevents bone loss in both thyroparathyroidectomized and ovariectomized rats, *J. Clin. Invest. 106*, 309−318.
21. Zhang, J., Feng, Y., and Forgac, M. (1994) Proton conduction and bafilomycin binding by the V_0 domain of the coated vesicle V-ATPase, *J. Biol. Chem. 269*, 23518−23523.
22. Crider, B. P., Xie, X.-S., and Stone, D. K. (1994) Bafilomycin inhibits proton flow through the H^+ channel of vacuolar proton pumps, *J. Biol. Chem. 269*, 17379−17381.
23. Rautiala, T. J., Koskinen, A. M. P., and Väänänen, H. K. (1993) Purification of vacuolar ATPase with bafilomycin C_1 affinity purified chromatography, *Biochem. Biophys. Res. Commun. 194*, 50−56.
24. Huss, M., Ingenhorst, G., Konig, S., Gassel, M., Drose, S., Zeeck, A., Altendorf, K., and Wieczorek, H. (2002) Concanamycin A, the specific inhibitor of V-ATPases, binds to the V_0 subunit c, *J. Biol. Chem. 277*, 40544−40548.
25. Bowman, B. J., and Bowman, E. J. (2002) Mutations in subunit c of the vacuolar ATPase confer resistance to bafilomycin and identify a conserved antibiotic binding site, *J. Biol. Chem. 277*, 3965−3972.
26. Harrison, M. A., Murray, J., Powell, B., Kim, Y.-I., Finbow, M. E., and Findlay, J. B. C. (1999) Helical interactions and membrane disposition of the 16-kDa proteolipid subunit of the vacuolar H^+-ATPase analyzed by cysteine replacement mutagenesis, *J. Biol. Chem. 274*, 25461−25470.
27. Pali, T., Whyteside, G., Dixon, N., Kee, T. P., Ball, S., Harrison, M. A., Findlay, J. B. C., Finbow, M. E., and Marsh, D. (2004) Interaction of inhibitors of the vacuolar H^+-ATPase with the transmembrane V-o-sector, *Biochemistry 43*, 12297−12305.
28. Ito, H., Fukuda, Y., Murata, K., and Kimura, A. (1983) Transformation of intact yeast-cells treated with alkali cations, *J. Bacteriol. 153*, 163−168.
29. Uchida, E., Ohsumi, Y., and Anraku, Y. (1985) Purification and properties of H^+-translocating, Mg^{2+}-adenosine triphosphatase from vacuolar membranes of *Saccharomyces cerevisiae*, *J. Biol. Chem. 260*, 1090−1095.
30. Jones, P. C., Harrison, M. A., Kim, Y.-I., Finbow, M. E., and Findlay, J. B. C. (1995) The first putative transmembrane helix of the 16 kDa proteolipid lines a pore in the V_0 sector of the vacuolar H^+-ATPase, *Biochem. J. 312*, 739−747.
31. Harrison, M. A., Powell, B., Finbow, M. E., and Findlay, J. B. C. (2000) Identification of lipid-accessible sites on the *Nephrops* 16-kDa proteolipid incorporated into a hybrid vacuolar H^+-ATPase: Site-directed labeling with N-(1-pyrenyl)cyclohexylcarbodiimide and fluorescence quenching analysis, *Biochemistry 39*, 7531−7537.
32. Parikh, H. H., McElwain, K., Balasubramanian, V., Leung, W., Wong, D., Morris, M. E., and Ramanathan, M. (2000) A rapid spectrofluorimetric technique for determining drug-serum protein binding suitable for high-throughput screening, *Pharm. Res. 17*, 632−637.
33. Bowman, E. J., Graham, L. A., Stevens, T. H., and Bowman, B. J. (2004) The bafilomycin/concanamycin binding site in subunit c of the V-ATPases from *Neurospora crassa* and *Saccharomyces cerevisiae*, *J. Biol. Chem. 279*, 33131−33138.
34. Harrison, M. A., Jones, P. C., Kim, Y.-I., Finbow, M. E., and Findlay, J. B. C. (1994) Functional properties of a hybrid vacuolar H^+-ATPase in *Saccharomyces* cells expressing the *Nephrops* 16-kDa proteolipid, *Eur. J. Biochem. 221*, 111−120.
35. Lakowicz, J. R. (1999) *Principles of fluorescence spectroscopy*, 2nd ed., Kluwer Academic/Plenum Publishers, New York.
36. Aoudia, M., and Zana, R. (1998) Aggregation behavior of sugar surfactants in aqueous solutions: Effects of temperature and the addition of nonionic polymers, *J. Colloid Interface Sci. 206*, 158−167.
37. Gagliardi, S., Rees, M., and Farina, C. (1999) Chemistry and structure activity relationships of bafilomycin a_1, a potent and selective inhibitor of the vacuolar H^+-ATPase, *Curr. Med. Chem. 6*, 1197−1212.
38. Kakinuma, Y., Yamato, I., and Murata, T. (1999) Structure and function of vacuolar Na^+-translocating ATPase in *Enterococcus hirae*, *J. Bioenerg. Biomembr. 31*, 7−14.
39. Girvin, M. E., Rastogi, V. K., Abildgaard, F., Markley, J. L., and Fillingame, R. H. (1998) Solution structure of the transmembrane H^+-transporting subunit c of the F_1F_0 ATP synthase, *Biochemistry 37*, 8817−8824.
40. Boyd, M. R., Farina, C., Belfiore, P., Gagliardi, S., Kim, J. W., Hayakawa, Y., Beutler, J. A., McKee, T. C., Bowman, B. J., and Bowman, E. J. (2001) Discovery of a novel antitumor benzolactone enamide class that selectively inhibits mammalian vacuolar-type (H^+)-ATPases, *J. Pharmacol. Exp. Ther. 297*, 114−120.
41. Murata, T., Yamato, I., Kakinuma, Y., Leslie, A. G. W., and Walker, J. E. (2005) Structure of the rotor of the V-type Na^+-ATPase from *Enterococcus hirae*, *Science 308*, 654−659.
42. Elston, T., Wang, H., and Oster, G. (1998) Energy transduction in ATP synthase, *Nature 391*, 510−513.
43. Rastogi, V. K., and Girvin, M. E. (1999) Structural changes linked to proton translocation by subunit c in the ATP synthase, *Nature 402*, 263−268.
44. Dixon, N., Pali, T., Kee, T. P., and Marsh, D. (2004) Spin-labelled vacuolar-ATPase inhibitors in lipid membranes, *Biochim. Biophys. Acta 1665*, 177−183.

BI051529H